KfK 3138
November 1981

Dependence of Dryout Heat Flux on Particle Diameter for Volume- and Bottom-Heated Debris Beds

L. Barleon, H. Werle
Institut für Neutronenphysik und Reaktortechnik
Institut für Reaktorbauelemente
Projekt Schneller Brüter

Kernforschungszentrum Karlsruhe

KERNFORSCHUNGSZENTRUM KARLSRUHE

Institut für Neutronenphysik und Reaktortechnik
Institut für Reaktorbauelemente
Projekt Schneller Brüter

KfK 3138

Dependence of Dryout Heat Flux on Particle Diameter for Volume- and Bottom-Heated Debris Beds

L. Barleon and H. Werle

Kernforschungszentrum Karlsruhe GmbH, Karlsruhe

Kernforschungszentrum Karlsruhe GmbH
ISSN 0303-4003

Contents

Dependence of Dryout Heat Flux on Particle Diameter for Volume- and Bottom-Heated Debris Beds

Abstract

The dependance of the dryout heat flux on the particle diameter has been investigated experimentally for volume- and bottom-heating in the particle diameter range 1 to 16 mm for Freon-113 and water. The experimental data for volume-heating are in agreement with theoretical models assuming turbulent flow, whereas the laminar models overpredict the dryout heat flux in this particle diameter range heavily. For bottom-heating the dryout heat flux shows the same particle diameter dependance as for volume-heating as long as the beds are in packed state, but the absolute values are about a factor of two lower. Beds may dryout at different heat fluxes depending on the state they assume.

Abhängigkeit des Dryout-Wärmeflusses vom Partikeldurchmesser für volumen- und bodenbeheizte Partikelbetten

Kurzfassung

Die Abhängigkeit des Dryout-Wärmeflusses vom Partikeldurchmesser bei Volumen- und Bodenheizung wurde im Partikeldurchmesserbereich 1 bis 16 mm für Freon-113 und Wasser experimentell untersucht. Die experimentellen Werte für Volumenheizung stimmen mit Modellen, die eine turbulente Strömung annehmen, überein, während die laminaren Modelle den Dryout-Wärmefluß in diesem Partikeldurchmesserbereich massiv überschätzen. Der Dryout-Wärmefluß für Bodenheizung zeigt dieselbe Abhängigkeit vom Partikeldurchmesser wie bei Volumenheizung solange die Betten kompakt sind, allerdings sind die Absolutwerte um etwa einen Faktor zwei kleiner. Die Betten können, je nachdem welchen Zustand sie einnehmen, bei unterschiedlichen Wärmeflüssen austrocknen.

1. INTRODUCTION

Decay heat removal from beds of fuel particles after a hypothetical core melt-down accident is an important aspect of safety, especially for liquid metal fast breeder reactors. Inadequate heat removal from the bed can lead to bed heatup, fuel melt, and attack on supporting structures. Considerable research has been performed to determine the conditions for dryout. According to theoretical models the dryout heat flux depends sensitively on the particle diameter, bit the exact dependance is quite different in the various models. The basic difference, what concerns larger particles (diameter > 1 mm) is, that Dhir and Catton /1/, Hardee and Nilson /2/ and Shires and Stevens /3/ assume laminar flow whereas Ostensen /4/ and Lipinski /5/ assume turbulent flow. According to the laminar models the dryout heat flux should be proportional to the square of the particle diameter, whereas the turbulent models predict a square root dependance. The models generally agree with available experimental data, which virtually all lie in the particle diameter range 0.3 to 1 mm. Only very few experimental data /3/ are available for larger particles. To check the theoretical models for larger particles, the dryout heat flux dependance of volume-heated beds with adiabatic bottom and bottom-heated beds on the particle diameter has been investigated systematically in the particle diameter range 1 to 16 mm for Freon-113 and (demineralized) water. Inductively heated stainless steel spheres were used in the volume-heated experiments. Bottom-heating of beds of glass spheres was accomplished by heating inductively either a steel ring which was soldered to a bottom plate made of copper or, alternatively, a shallow bed of stainless steel spheres.

2. EXPERIMENTS AND RESULTS

2.1 Experimental set-up

The experimental set-up for volume-heating is shown in Fig. 1. The particulate bed is contained in a cylindrical, double-wall quartz glass vessel (inner diameter 8 cm, bottom area 50.27 cm^2). The (adiabatic) bottom of the vessel consists of a thick plate. Above the plate there is a 5 mm thick glass or Al_2O_3 plate to protect the plate from the hot bed and to equalize the bed temperatures at the bottom. The bed is heated volumetrically by an induction coil (inner diameter 10,5cm height 13 cm, number of windings 9) connected to a 400 kHz generator.

The heat is removed from the top of the bed via the cooling liquid (Freon-113 or distilled water) with a heat exchanger consisting of a helical copper tube. The distance between the top of the bed and the lower end of the heat exchanger (HX) was larger than 10 cm. If the liquid level is high the heat exchanger is immersed in the liquid. The heat transfer between the bed and the heat exchanger is then partly by convection in the liquid and the liquid pool may by subcooled. If the liquid level is below the heat exchanger the bed power is transfered by vaporization and recondensation to the heat exchanger and the pool is saturated.

The power removed by the heat exchanger was determined from the measured volumetric flow rate $\dot{V}$ and the temperature increase ΔT_{HX} of the cooling water according to

$$P_{HX} = c \cdot \rho \cdot \dot{V} \cdot \Delta T_{HX} \qquad (1)$$

$c = 4.18$ J/g°C and $\rho = 1.00$ g/cm^3 are the specific heat and the density of the cooling water, respectively. The flowmeter was connected to the heat exchanger inlet. For the dryout measurements the temperature of the cooling water at the heat exchanger inlet was 14 ± 2 °C. The flowmeters have been calibrated at 14 °C. During the dryout measurements the flow rate was kept constant. The accuracy of the flow rate measurements is estimated to be $\pm$ 3 %. The error in ΔT_{HX} was sometimes up to $\pm$ 0,5 °C, normally about $\pm$ 0.2 °C.

The power loss through the vessel has been estimated from measurements with a similar vessel /6/ to be about 1 $\frac{W}{^{o}C}$ ($T_{pool} - T_{environment}$). For water the power losses due to vaporization through the open top of the vessel are well below 1 %. For Freon the vaporization losses might be remarkable if the heat exchanger is not very efficient. In a first series of investigations, covering the Freon dryout measurements for 2 and 3 mm Ø steel spheres, a single-helix heat exchanger has been used. The vaporization losses have been measured to be < 1 % for both particle sizes. Later on, covering the Freon dryout measurements of the larger particles, a double-helix heat exchanger with an additional copper top plate was used to keep the Freon vaporization losses sufficiently small. The measured dryout heat fluxes have been corrected for these heat losses.

Temperatures were measured with thermocouples using a data logger. The temperature of the liquid pool above the bed was normally measured at three positions:

About 1 and 2 cm above the bed surface and at the center of the heat exchanger. Bed temperatures were normally measured at three horizontal planes: About 2 mm above the bottom, in the center and about 10 mm below the bed surface. At least three thermocouples were available at each of these planes. Details on the thermocouple (TC) arrangements are given in Fig. 2. The different arrangements are identified by the data, when they were first used (year/month/day). For the smaller particles (diameter ≤ 4.76 mm) the thermocouples were located in between the particles, for the larger particles they were in a 1 mm drilling within the particles (Fig. 2). The thermocouples were running vertically from above into the bed region. After fixing the thermocouples in the bed region the particles were poured into the vessel.

In the volume-heated runs, the particles were stainless steel spheres with 2, 3, 4.76, 7.94, 10 and 15.88 mm diameter respectively. To prevent circular currents extending over larger bed regions, the surface of the spheres has been oxydized.

2.2 Porosity measurements

The porosity ε of the 8 cm diameter beds (height 6-9 cm) was determined during the dryout measurements with the fixed thermocouple arrangement in the bed region and afterwards with and without thermocouple arrangement. ε was measured by filling in the dry bed from below through a tube a certain liquid volume ΔV_{liquid} and observing the rise ΔH of the liquid level in the filling tube (Fig. 3). The porosity is then calculated according to

$$\varepsilon = V_{void}/V_{bed} = \frac{\Delta V_{liquid}}{F_{vessel} \cdot \Delta H} - \frac{F_{tube}}{F_{vessel}} \qquad (2)$$

F_{vessel} and F_{tube} are the areas of the vessel and the filling tube, respectively. To exclude boundary effects at the bottom and the surface, the liquid level was at least one particle diameter above the bottom or below the top of the bed before and after adding the liquid, respectively. The total error of the porosity is estimated to be < 3 %, where 1 % is due to uncertainties in ΔV_{liquid} and 2 % due to uncertainties in ΔH.

The results are shown in Fig. 3. The porosity values are generally reproducible within the estimated error. No systematic differences are seen if either Freon or water is used. Moreover, the porosity values with and without thermocouple arrangements are equal within the experimental error. Attempts to compress the beds has also no detectable influence on the porosity. The porosity increases with the particle diameter. The measured values have been fitted by a straight line. The error in the recommend ε-values is estimated to be about $\pm$ 1 %.

2.3 Beds of volume-heated stainless steel spheres with adiabatic bottom

For these measurements the vertical center of the induction coil and of the particulate bed were at the same height to get a homogeneous power density distribution in the bed.

2.3.1 Power calibration

As has been discussed in section 2.1, the heat exchanger power should be equal within about ± 5 % to the power generated in the bed. It was tried to check this relation by measuring the bed power via the average rate of rise in the bed temperature $\overline{\Delta T/\Delta t}_{bed}$ when a constant high-frequency power was applied. For these measurements the bed was just covered by water. The bed power was calculated according to

$$P_{bed} = \left[(V \cdot \rho \cdot c)_{water} + (1-\varepsilon) H \cdot F \ (\rho \cdot c)\right] \cdot \overline{\Delta T/\Delta t}_{bed} \quad (3)$$

The first term is the heat capacity of the water, H and F are the height and the bottom area of the bed, ρ and c are the density and the specific heat. To determine $\overline{\Delta T/\Delta t}_{bed}$ the readings of the bed thermocouples (TC) were averaged.

This check was performed three times, once for a bed of 7.94 mm spheres and two times for 15.88 mm spheres. It was found that P_{HX} and P_{bed} agree in the average only within about 20 %. The main reason for this discrepancy is probably the uncertainty in $\overline{\Delta T/\Delta t}_{bed}$. This uncertainty is mainly due to differences in the ΔT/Δt-values of the various thermocouples, which are probably caused by convective movements in the water.

2.3.2 Homogeneity of power density

In the voided (air-filled) beds the thermal conductivity is very small. If a constant high-frequency power is suddenly applied to the bed, the temperature rises linearly with time and the power density q is proportional to the initial local temperature gradient. ΔT/Δt-values are shown for the three instrumented horizontal planes (bottom, center, top) as a function of the bed radius in Fig. 4. The values scatter in the average by about ± 10 % around the mean value. This scattering is probably caused by the fact, that only the surface of the spheres is heated and therefore the temperature gradients measured with the thermocouples depend sensitively on the local arrangement of the spheres (when the thermocouples are between the spheres) or on the exact position of the thermocouple within the spheres.

For the whole range of sphere diameters (2-15.88 mm) no systematic variation of the power density with the radial or axial position within the bed can be seen. If there are any systematic power density inhomogeneities, they are well below ± 10 %. A similar result was found earlier with 54 mm diameter of 2 and 3 mm stainless steel spheres /6/.

2.3.3 Dryout measurements

Normally the following procedure was used to determine the dryout heat flux j_{do}: First a rough value of j_{do} was obtained by increasing the high-frequency power, which is controlled by a potentiometer (Pot), in quite large steps. Afterwards the dryout region was investigated in detail by increasing the power by small steps starting well below dryout. This second step was normally repeated several times. After each power increase, the system was allowed to achieve stationary conditions. This took normally some minutes and was controlled by the thermocouple readings. When stationary conditions were achieved, the thermocouple signals were registered at least three times. Over a large power range the bed temperatures stay near the boiling point. Dryout is indicated if the signals of one or more thermocouples begin to rise strongly with the power, achieving values definitely above the boiling temperature of the liquid. For Freon-113 (boiling temperature 47.7 °C) the dryout temperature limit corresponds to about 70, and for water to about 130 °C. For the different runs the bed height, the type of heat exchanger and the thermocouple (TC) arrangement is specified. In some runs it was tried to control the state of the liquid (saturated or subcoold) by the amount of liquid filled into the vessel. It can be seen that it is very difficult to get subcooled conditions for Freon. The pool temperatures are always above or very near the boiling temperature. Therefore for Freon the state of the liquid generally may be assumed to be saturated.

The determination of the dryout heat flux j_{do} is illustrated in Fig. 5, where the measured heat flux j (average over at least three values) is shown as a function of the power controlling potentiometer setting (Pot). The measured values are fitted by a smooth line. From the measured dryout Pot-value, j_{do} is then determined from this smooth line. Using the fitted instead of the direct measured j_{do} value reduces the statistical uncertainty considerably. The error in j_{do} is estimated from the uncertainty in the smooth line fit (this accounts for statistical uncertainty of the power determination), from the uncertainty in the Pot-value corresponding to dryout (estimated from repeated runs) and from the uncertainties in the heat exchanger flow rate and temperature rise.

The measured j_{do} values have been corrected for the radial heat losses and for vaporization losses. The corrections are very small (< 3 %).

It should be noticed that after dryout the temperatures might be very high, but are generally stationary at a fixed power level. Some runs (especially with water) had to be terminated before reaching stationary conditions not to destroy the vessel by too high temperatures.

For the bed of 2 mm spheres in Freon, a strong movement of the spheres at the bed surface was observed. This led to remarkable deformations of the original horizontal surface during the dryout measurements. For the other dryout measurements no movement of the steel spheres was observed.

For the investigations with water the corrections of the dryout heat flux for the vaporization losses are negligible and those for the radial heat losses are very small. For the smaller spheres dryout was indicated, as was generally the case for Freon-113, by the thermocouples. In one run with the 7.94 mm and in most runs with the 15.88 mm spheres, dryout was not indicated by the thermocouples but by glowing in the bed. Although with water it was possible to achieve subcooling up to about 40 ^{o}C (for the 7.94 mm spheres), no systemtic dependence of j_{do} on the subcooling can be deduced from the measurements. This is not unexpected because if the bed characteristics and the overall flow

pattern are not affected by the subcooling, $j_{do} \sim 1 + \frac{c}{h} \cdot (T_{boil}-T_{pool})$ where c and h are the specific heat and heat of vaporization of the liquid and $(T_{boil}-T_{pool})$ is the subcooling. This relation predicts only a 7 % increase in j_{do} for 40 °C subcooling as compared to the value for saturated conditions. The effect of subcooling is therefore small compared to the scattering in the experimental dryout values. As was the case for Freon-113, also for water the dryout heat fluxes may therefore be assumed to refer to saturated conditions.

The variation of heat flux j and bed temperatures T with time are shown for some runs in Fig. 6 for Freon-113 and in Fig. 7 for water. Only those thermocouple signals are plotted for which dryout was observed. Generally, for Freon-113 and water, after a stepwise variation of the heat flux, the temperatures change rapidly (within seconds) to new stationary values. Especially for water, relatively high temperatures (> 500 °C) may be achieved after dryout.

2.4 Dryout in bottom-heated beds

"Bottom heating" of stainless steel spheres was simulated by lowering the center of the induction coil by about 7 cm as compared to the center of the bed. The corresponding vertical power density distribution for a bed of 7.94 mm diameter spheres is shown in Fig. 8. The power density decreases about exponentially in the vertical direction to about 30 % at the center as compared to the bottom.

In addition, clean bottom-heated experiments have been performed with glass balls. The container was the same as for the volume-heated experiments. The balls were not exactly spherical, but the deviations from spheres are small (< 6 %). Also the size was not exactly equal. For the smaller balls ($\leq$ 3.1 mm diameter) the width of the particle size distribution amounts to about 10 % of the average diameter, for the larger particles this figure is even less. The porosity has been measured as described in 2.2.

Because the porosity may be influenced by shape factors (which might be different for the various particle sizes), the measured values have not been fitted by a smooth line. The measured average is used for further evaluations.

For all bottom-heated experiments the double-helix heat exchanger was used. Two different heated bottoms were used: A flat copper plate and a thin layer of stainless steel spheres, both inductively heated.

2.4.1 Copper plate

Bottom heating was accomplished with an inductively heated steel ring which was soldered to a massive copper plate (Fig. 9). The seal between the copper plate and the glass vessel was not completely tight. Some liquid drained through the seal, but is is estimated that the enhancement of the heat flux caused by this effect is negligible. Dryout heat fluxes were determined with this set-up for Freon-113 and water for the bare copper plate (Zuber heat flux) and for 5.2 mm diameter glass balls as a function of the bed height. Dryout was indicated by the three thermocouples located at different radial positions within the copper plate 2 mm below the surface. The three thermocouple readings were before and after dryout within $2^{\circ}C$ equal. The results are shown in Fig. 9. Symbols with arrow down indicate that the measured value is an upper limit, those with an arrow up indicate that is a lower limit. Movement of the particles was noticed with water and small bed heights.

In the following series of experiments with the copper plate the dryout heat flux dependance on the particle size was determined for deep beds (bed height 6 ± 0.5 cm) with Freon-113 and water as coolant. For these experiments the set-up (Fig. 10) has been improved by inserting a tight Teflon seal in the gap between the copper plate and the wall of the glass container. Dryout was again indicated by the thermocouples in the copper plate. Generally, at dryout the readings of the three thermocouples were within $2^{\circ}C$ equal. Only for water and larger particles (diameter ≥ 5.2 mm) differences of up to $10^{\circ}C$ were noticed.

2.4.2 Thin layer of stainless steel spheres

In this series of experiments the heated copper plate was replaced by a thin (2 - 3 cm) layer of inductively heated stainless steel spheres (Fig. 11). The bed height of the overlaying glass balls was normally 6, in some cases up to 9 cm. The arrangement of the thermocouples is also shown in Fig. 11. The dryout heat flux of the bottom-heated glass beds was investigated as a function of the particle diameter. To ensure that the dryout is determined from the glass bed and not from the stainless steel bed, the diameter of the stainless steel spheres was generally larger than that of the glass particles. In addition for the 3.1 mm diameter glass balls two different bottom layers were used. Dryout was normally indicated by the three thermocouples located in the heated steel bed. For water and larger particles, dryout was sometimes indicated also by glowing or only by glowing in the steel bed. In one run only, also one thermocouple in the glass bed was definitely above the boiling point.

3. DISCUSSION OF RESULTS

3.1 Dryout in beds of volume-heated stainless steel spheres with adiabatic bottom

As has been discussed earlier, subcooling effects are negligible. In addition, essentially no particle movement or vapor channel formation have been observed with these beds. Moreover, experimental investigations /6/ with 2 and 3 mm stainless steel spheres in Freon-113 with bed heights from 2 to 6 cm revealed no bed height dependance of the dryout heat flux. Therefore the experimental data may be put together and refer to deep, packed beds and saturated liquids.

The dryout heat flux depends strongly on the porosity of the beds. According to /5/ for particles larger than about 1 mm $j_{do} \sim \left(\frac{\varepsilon^3}{1-\varepsilon} \right)^{1/2}$. For comparison with theoretical models the experimental values have been normalized to $\varepsilon = 0.40$ using this relation. The corrections are 27 % at the most (for the 15.88 mm partices).

The normalized dryout heat fluxes are shown in Fig. 12 as a function of the particle diameter. The values where one, two or ≥ three thermocouples went into dryout or dryout was indicated by glowing are not very different. Therefore the heat fluxes corresponding to complete dryout are probably not much higher. This is favorable with respect to comparison with theory, because it is generally not obvious if the theoretical dryout fluxes refer to beginning or complete dryout. The experimental heat fluxes for initial dryout have been fitted by a smooth curve. It can be seen that the experimental curve agrees quite well the relation $j_{do} \sim d^{1/2}$ (d particle diameter).

In Fig. 13 the experimental dryout heat fluxes are compared with measured values of Shires and Stevens /3/ for water and calculated data /5/ using different theoretical models. The values of /3/ have not been normalized because no exact ε-values are given, but the porosity probably was about 0.40. If both experimental data sets for water are fitted by smooth lines, the two sets agree within about 30 %, which is satisfactory in view of the different heating methods (direct electrical heating of the metalic particles by electrods is used in /3/) and the uncertainties in ε. Nevertheless the difference between the two experimental sets is about two times larger than the error we would attribute to the fit through our data.

What concerns the comparison with theoretical prediction, Fig. 13 shows that for water both, the model of Ostensen and that of Lipinski, are in excellent agreement (practical within our estimated error) with our experimental data, whereas the other models overestimate the dryout heat flux for the largest particles (15.88 mm diameter) by nearly two orders of magnitude (Ostensen and Lipinski essentially added a turbulent term in the equation of motion). It has been shown /5/, that the Lipinski model agrees also reasonably well with numerous experimental data in the particle diameter range 0.3 to 1 mm, whereas the Ostensen model is generally too high in this range. For Freon-113 the agreement with Lipinski's prediction seems to be even better than for water. The overestimation of the laminar models is similar as for water.

In Fig. 14 the experimental data for water are compared with more detailed calculations based on Lipinski's model /5/, showing also the effect of different bed heights. According to the calculations, for the particle diameter range investigated here, the dependance of the dryout heat flux on the bed height is small for water and negligible for Freon-113, in agreement with experimental findings /6/. Therefore, the procedure of putting together the experimental data for the different bed heights (6 to 9 cm) seems to be justified.

In the theoretical models the beds are normally assumed to be radially unrestricted. On the other side, the experiments (especially in-pile experiments) are restricted to diameters of about 10 cm and the desired radial infinity is approximated by adiabatic walls. The question then arises what is the minimum bed diameter to achieve results which are representative for radially unlimited beds. Below are compared the dryout fluxes measured here with those found with 5.4 cm diameter beds and adiabatic bottom /6/, both normalized to a porosity of 0.40.

Bed		Dryout heat flux (W/cm^2), Freon-113, ε = 0.40					
		2 Part. diam (mm) 3					
		Number of thermocouples in dryout					
Diam. (cm)	Height	1	2	3	1	2	3
8	8	26	36	38	30	34	-
5.4	6	20	20	22	26	32	36

As can be seen from Fig. 12 the 5.4 cm bed diameter data agree essentially with the curve fitted to the 8 cm bed diameter data. It should be mentioned that the radial heat losses were very small (less than 3 % in both cases). From this it may be concluded that for small radial heat losses a bed diameter of 5 cm seems sufficient for dryout investigations of particles with diameters less than 3 mm.

The location of the dryout zone is shown in Fig. 15 (z axial, r radial coordinate). The black symbols indicate where the dryout was first observed, the open symbols the extension of the dryout zone if the power was further increased. The location of the dryout is generally not reproducible in repeated

dryout runs with the same bed. In a previous investigation /6/ movements of the dryout zone have been observed at constant power. These observations indicate that the generation and the local distribution of the dryout zone are stochastic processes. This stochastic nature is reflected in Fig. 15. It is very difficult to condense the data of Fig. 15 to some useful general trends. It may be mentioned that for Freon-113 dryout never started at the bottom and for water this happened only occasionally for the 2 mm diameter particles. These results are not contradictory to the observations in /7/ that for particles of 2, 1.2 and 0.68 mm diameter in water, dryout generally occurs near the bottom.

3.2 Dryout in bottom-heated beds

The dryout heat fluxes for the pseudo "bottom-heated" beds of stainless steel spheres are lower than the corresponding heat fluxes for uniform power density (volume heating). The difference amounts to about 30 % (Fig. 12). A theoretical interpretation is not possible at the moment. However, one may conclude that even a strong inhomogeneity in the power density has only a small effect on the dryout heat flux. Furthermore it is interesting, that even with a strong concentration of the power density at the bottom (Fig. 8), dryout did not start at the bottom but in the central region.

What concerns the experiments with the heated copper plate, one may first compare the bare plate values with Zuber's prediction /8/

$$j_z = \frac{\pi}{24}\,\rho_v^{1/2}(g\rho_\ell\sigma)^{1/4}\cdot h \qquad (4)$$

where ρ_v and ρ_ℓ are the vapour and liquid density, g the gravitational acceleration, σ the surface tension and h the heat of vaporization. With $\rho_v = 7.4\cdot10^{-3}$ g/cm^3, $\rho_\ell = 1.51$ g/cm^3, $\sigma = 13$ g/s^2 and $h = 144.6$ J/g for Freon-113 and $\rho_v = 6.0\cdot10^{-4}$ g/cm^3, $\rho_\ell = 0.96$ g/cm^3, $\sigma = 59$ g/s^2 and $h = 2257$ J/g for water one gets Zuber heat fluxes of 19.2 and 111 W/cm^2 for Freon-113 and water, respectively, whereas the experimental values are 33±6, 29±6 30 ± 5, 27 ± 5 for Freon-113 and > 147 W/cm^2 for water. It is not surprising that the experimental values are somewhat higher

than Zuber's prediction, because surface roughness increases the dryout heat flux and the copper plate was probably not sufficiently well machined.

If the copper plate is covered with 5.2 mm glass balls (Fig. 9), the dryout heat flux decreases initially strongly with increasing bed height from the bare plate value. For bed heights smaller than about 2 cm, strong movement of the balls is observed. Above this critical bed height there is no movement and the dryout heat flux is essentially independant of the bed height.

What concerns the measurements with a shallow ($\leq$ 3 cm) bottom layer of steel spheres one may first compare the dryout heat fluxes for Freon-113 without glass balls with the deep ($\geq$ 6 cm) bed data (Fig. 12). Within about ± 10 %, with corresponds to the experimental error, the values are equal for the particle sizes investigated (2 - 10 mm diameter), confirming earlier findings /6/.

In Fig. 16 and 17 the dryout heat fluxes for the bottom-heated glass balls are compared with those for the volume-heated steel spheres (for volume-heating only the heat fluxes corresponding to initial dryout are shown). The values of each of the three data sets are connected by smooth lines to guide the eye.

First one finds that the dryout heat fluxes for the glass balls are generally about a factor three lower when heated with the copper plate as compared to those with steel sphere heating. This shows that the dryout heat fluxes with the copper plate are not characteristic for the beds of glass balls. It is supposed that these values reflect the characteristics of the copper plate - glass bed interface. No theoretical description is available for such a configuration.

Comparing now the bottom-heated (glass over steel) with the volume-heated values one may distinguish two regions. For particle diameters $d \geq 3$ mm the two data sets show, for Freon-113 as well as for water, nearly the same dependance ($j_{do} \sim d^{1/2}$), however the absolute values are lower for bottom-heating than for volume-heating. In the average the ratio of bottom-to-volume heated values is about 0.6 for Freon-113 and 0.5 for water.

These ratios are consistent with a value of 0.5 deduced by Dhir and Catton from theoretical considerations based on laminar flow and verified experimentally /1/. Following the considerations of Dhir and Catton and assuming turbulent flow one gets a ratio of $1/\sqrt{3} = 0.58$. This number, too, is consistent with our experimental data. One comment should be added in this context: To arrive at different heat fluxes for bottom- and volume-heating it is necessary to release the assumption of pressure equilibrium between the vapour and the liquid phase in each horizontal plane. Instead one demands pressure equilibrium only at the bed surface. It is questionable, how the violation of the physical evident assumption of local pressure equilibrium can be justified.

For particle diameters < 3 mm the behaviour of the glass beds is very complex. This complexity is attributed to particle movement which may cause changes in the bed characteristics. These speculations are confirmed by the observation that for the same bed in two cases quite different dryout heat fluxes, obviously corresponding to different bed types, were found: For the bed of 1 mm diameter particles in Freon-113 heated with the copper plate movement in the whole bed or only in the upper part was observed. The dryout heat fluxes were 6.4 and 2.7 W/cm^2, respectively. For the bed of 2 mm diameter particles in water heated by the steel spheres strong particle movement combined with large diameter ($\simeq$ 1 cm), stable vapour channels (void of particles) or no particle movement was observed. The dryout heat fluxes were 66 and $\simeq$ 6 W/cm^2, respectively. Which state of the bed is achieved depends, amoung other parameters, also on the power history: Generally it was observed that with a slow power increase the high dryout state was achieved, whereas with a fast power increase the bed stays in the packed, low dryout state. The observation that the same bed may assume different states (packed, non-channeled or channeled) has also been made in Sandia's inpile experiment D-4 /9/.

The bed type obviously has a strong influence on the dryout heat flux. Our observations concerning the different bed types may be summarized as follows: If there is no particle movement the beds stay in a packed state. This was the case for the high density steel spheres in water and in Freon-113 for steel spheres

with diameter > 3 mm. For diameters $\leq$ 3 mm movement at the bed top was observed. In water for the low density glass balls movement at the bed top was observed for diameters $\geq$ 3 mm and in the whole bed for the smaller diameter glass balls. In Freon-113 for the glass balls movement at the bed top was observed for diameters < 5 mm and for 1 mm diameter over the whole bed. The particle movement changes the state of the bed from packed to non-packed. But the non-packed state is quite different for water and Freon-113: In water, large ($\simeq$ 10 mm diameter), empty (particle-free), stable vapor channels develop. Such particle-free channels were not observed with Freon-113, although the vapor is released from the bed surface from more or less stable centres. The formation of particle-free vapor channels in water is probably due to the high surface tension, which causes the particles to stick together.

From these observations it is concluded that there may exist different types of non-packed beds. Therefore the hitherto used descriptions (deep, shallow /1/; packed, channeled /9/) are not sufficient. The type of bed and correspondingly the dryout heat flux depend, among other parameters on the density, size, shape of the particles, on the wetting behaviour, surface tension and heat of vaporization of the liquid, the bed height and the power history.

4. CONCLUSIONS

- The dryout heat flux for volume- and bottom-heated particulate beds has been investigated in the particle diameter range 1 to 16 mm for Freon-113 and water. The experimental values for volume-heating agree well with the turbulent models of Ostensen and Lipinski, whereas the laminar models are far too high for these relatively large particles. Lipinski's prediction is also in reasonable good agreement with data for smaller particles (0.3 to 1 mm) where Ostensen's model is too high. Therefore of the available models only Lipinski's is in reasonable agreement with experimental data over the whole interesting particle diameter range.
- The dryout heat flux for the beds of glass balls heated by a shallow bottom layer of stainless steel spheres shows for

larger particles ($d \geq 3$ mm) nearly the same particle diameter dependance as for volume-heating. The absolute values however are about a factor of two lower, which may be explained in the context of the available theoretical models, by demanding pressure equilibrium between the liquid and vapor phase only at the bed surface. For smaller particle diameters ($d < 3$ mm) the behaviour of the dryout heat flux gets very complicated because the beds may change from a packed to a non-packed state.

- When bottom-heating is provided by a plane copper plate the dryout heat fluxes are even a factor four lower than volume-heating. This indicates that for such a configuration the measured dryout flux is not characteristic for the bed of glass balls but for the bed-plate interface.
- There are two areas which are not sufficiently well understood and need further investigations: 1) Behaviour during and after dryout, especially location, growth and temperature of the dryout zone. 2) Parameters which determine the different types of non-packed beds and relation to dryout heat flux.
- Further interesting results are:

  1) Liquid subcooling has only a very small influence on the dryout heat flux if the bed type is unchanged.

  2) The same bed may dryout at very different heat fluxes, depending on the state of the bed, which in turn is governed by the preceding bed history (power trace).

  3) If the radial heat losses are small, a bed diameter of about 5 cm seems to be sufficiently large for dryout investigations of particles with diameter less than 3 mm.

References

/1/ V.K. Dhir and I. Catton, "Study of Dryout Heat Fluxes in Beds of Inductively Heated Particles," NUREG-0262 USNRC, Los Angeles (June 77)

/2/ H.C. Hardee and R.H. Nilson, Nucl. Sci. Eng. 63, 119 (1977)

/3/ G.L. Shires and G.F. Stevens, "Dryout During Boiling in Heated Particulate Beds," AEEW-M1779, UKAEA, Winfrith,

/4/ R. W. Ostensen, "Advanced Reactor Safety Research Program, Quarterly Report October-December 1979", Sandia Laboratories, NUREG/CR-1572, p. 114 (1980)

/5/ R.J. Lipinski, "Particle Bed Dryout", Sandia Laboratories, Albuquerque, NM, to be published

/6/ L. Barleon, H. Werle "Debris Bed Investigations with Adiabatic and Cooled Bottom," Ninth Meet. Liquid Metal Boiling Working Group (LMBWG), Rome (June 1980)

/7/ R. Trenberth, G.F. Stevens, "An Experimental Study of Boiling Heat Transfer and Dryout in Heated Particulate Beds," AEEW-R1342, UKAEA, Winfrith, UK (1980)

/8/ N. Zuber, "Hydrodynamic Aspects of Boiling Heat Transfer", AEC Report No. AECU-4439, Physics and Mathematics, 1959

/9/ M. Schwarz, J.E. Gronager, R.J. Lipinski, "Particle-Bed Heat Removal with Subcooled Sodium: D4 Analysis," ANS Trans. 35, 357 (1980)

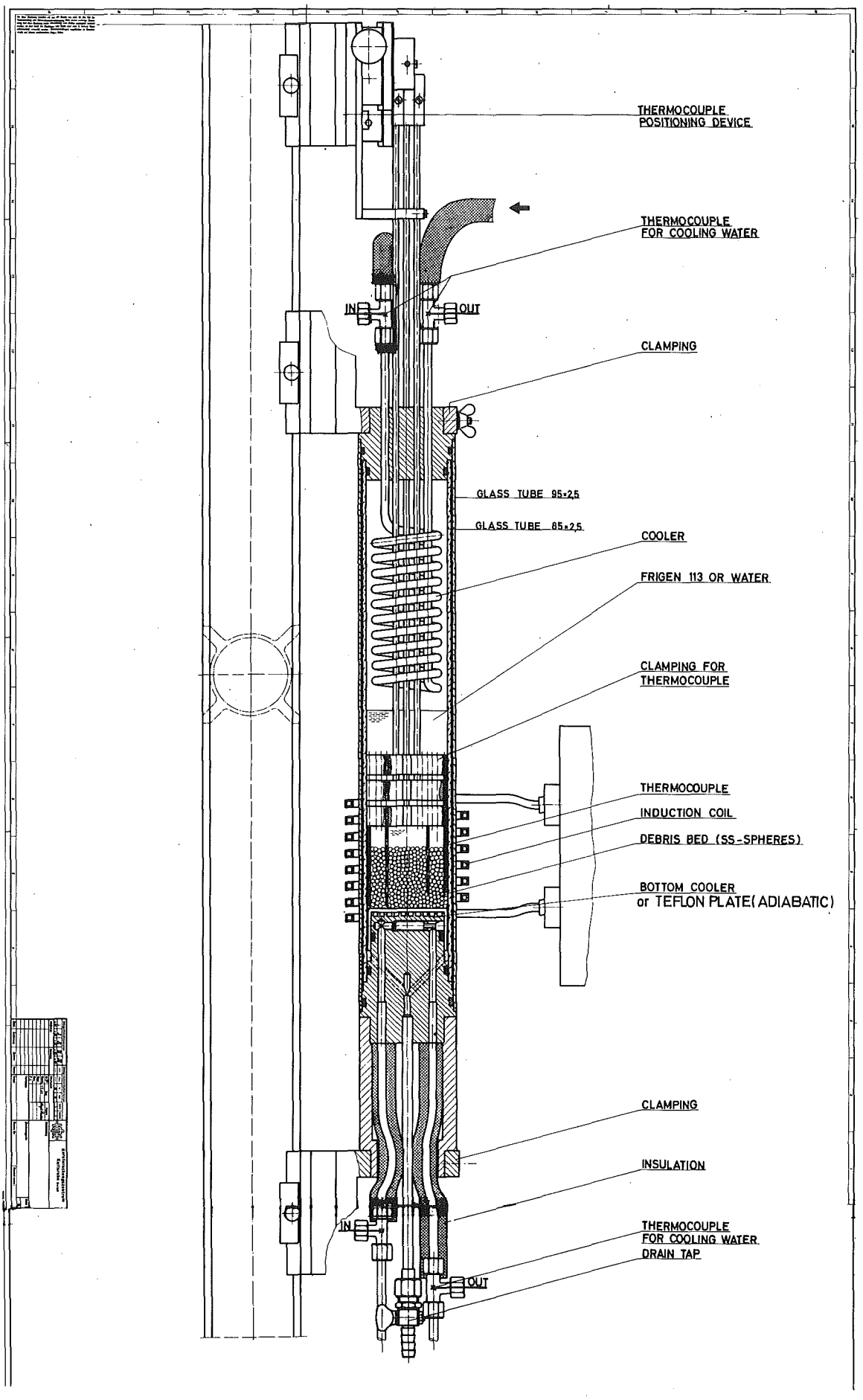

Fig. 1 Set-up for volume-heated beds

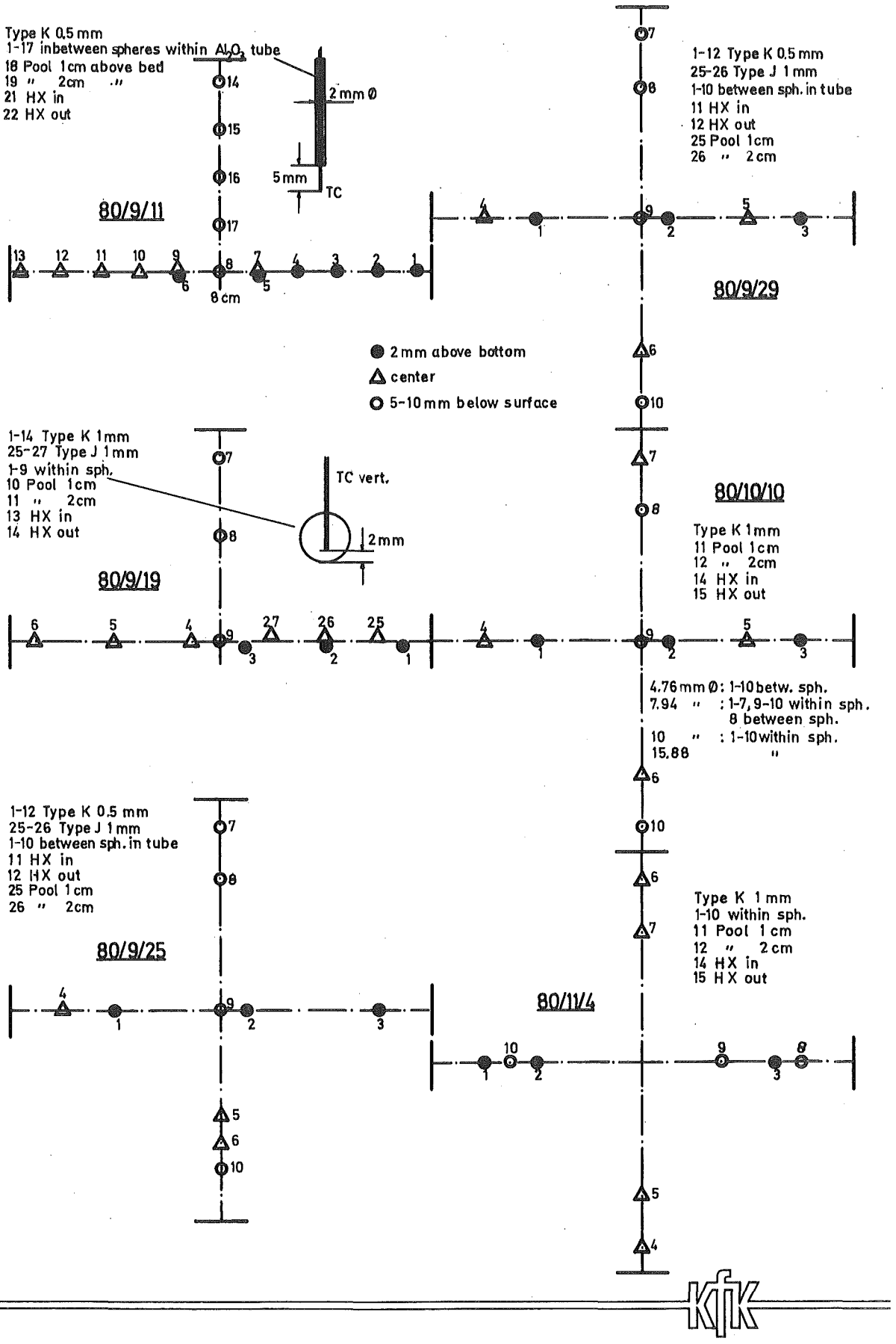

Fig. 2 Thermocouple arrangements for volume-heated beds

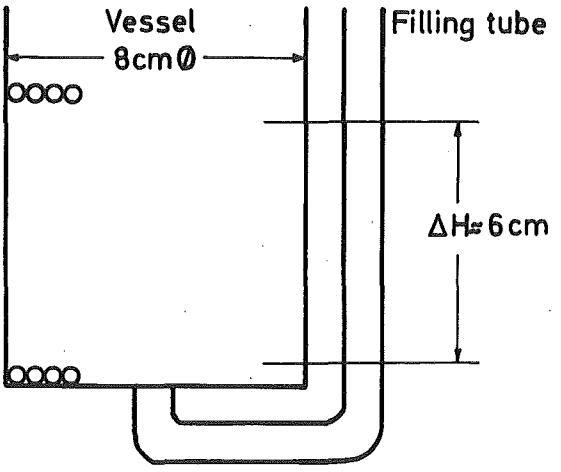

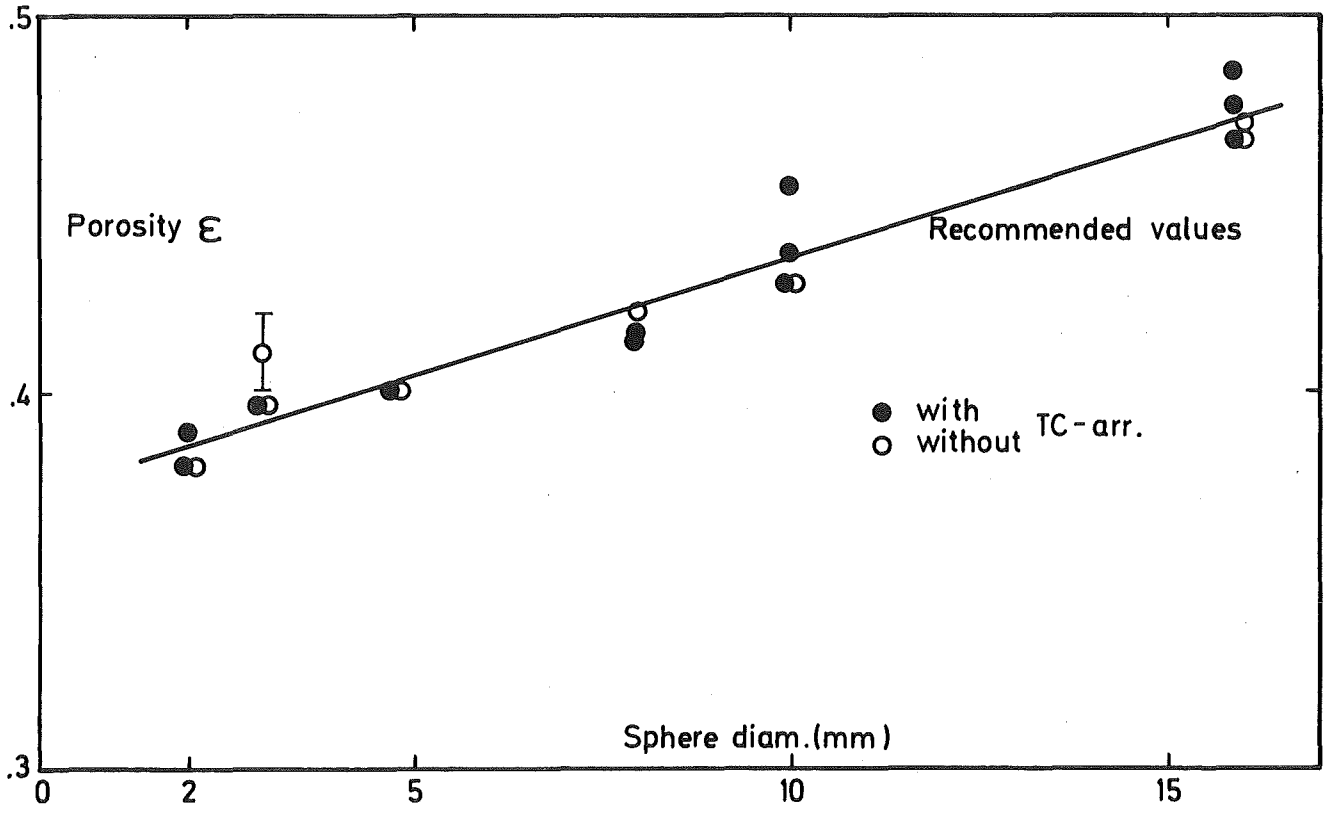

Fig. 3 Porosity (ε) of 8 cm diameter beds (height 6-9cm) of stainless steel spheres

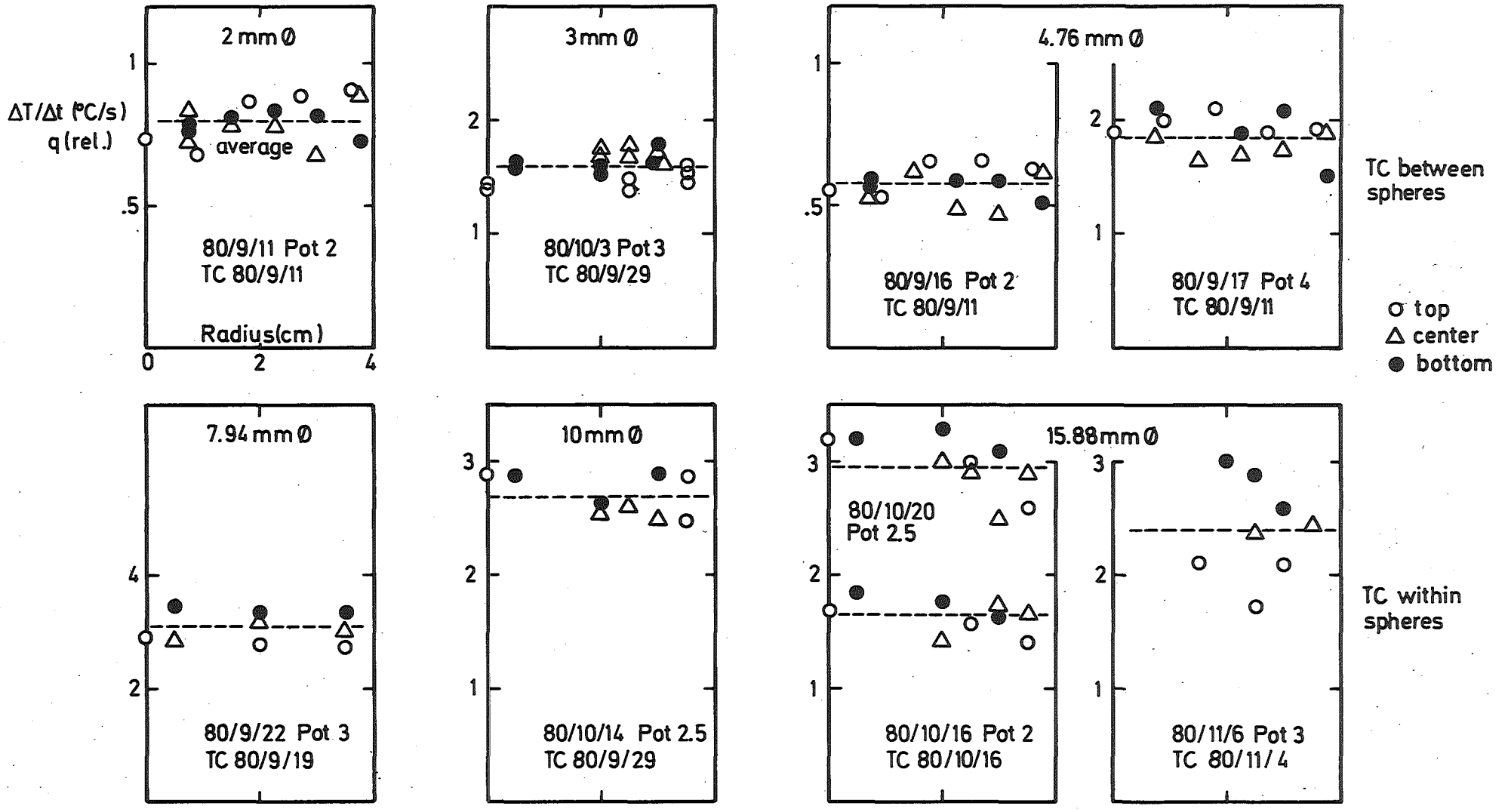

Fig. 4 Power density distribution in volume-heated 8 cm diameter beds (height 6-8 cm) of stainless steel spheres

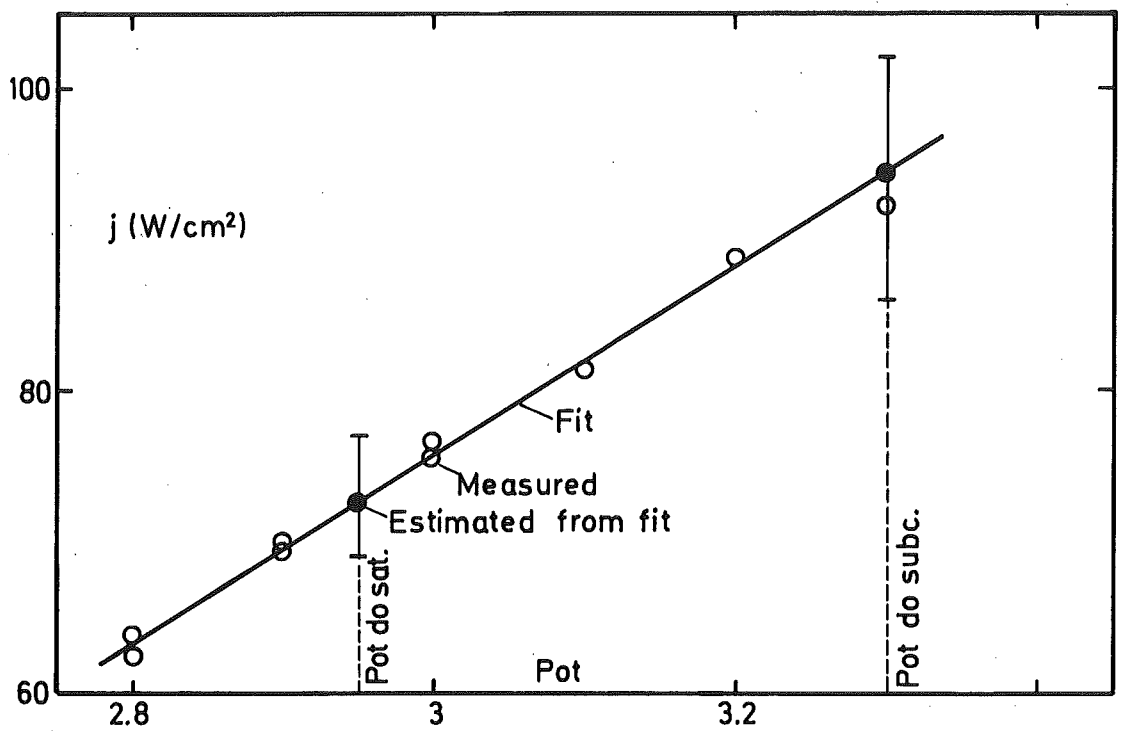

Fig. 5 Determination of dryout heat flux (Freon-113, 10 mm SS, Run 80/10/14/)

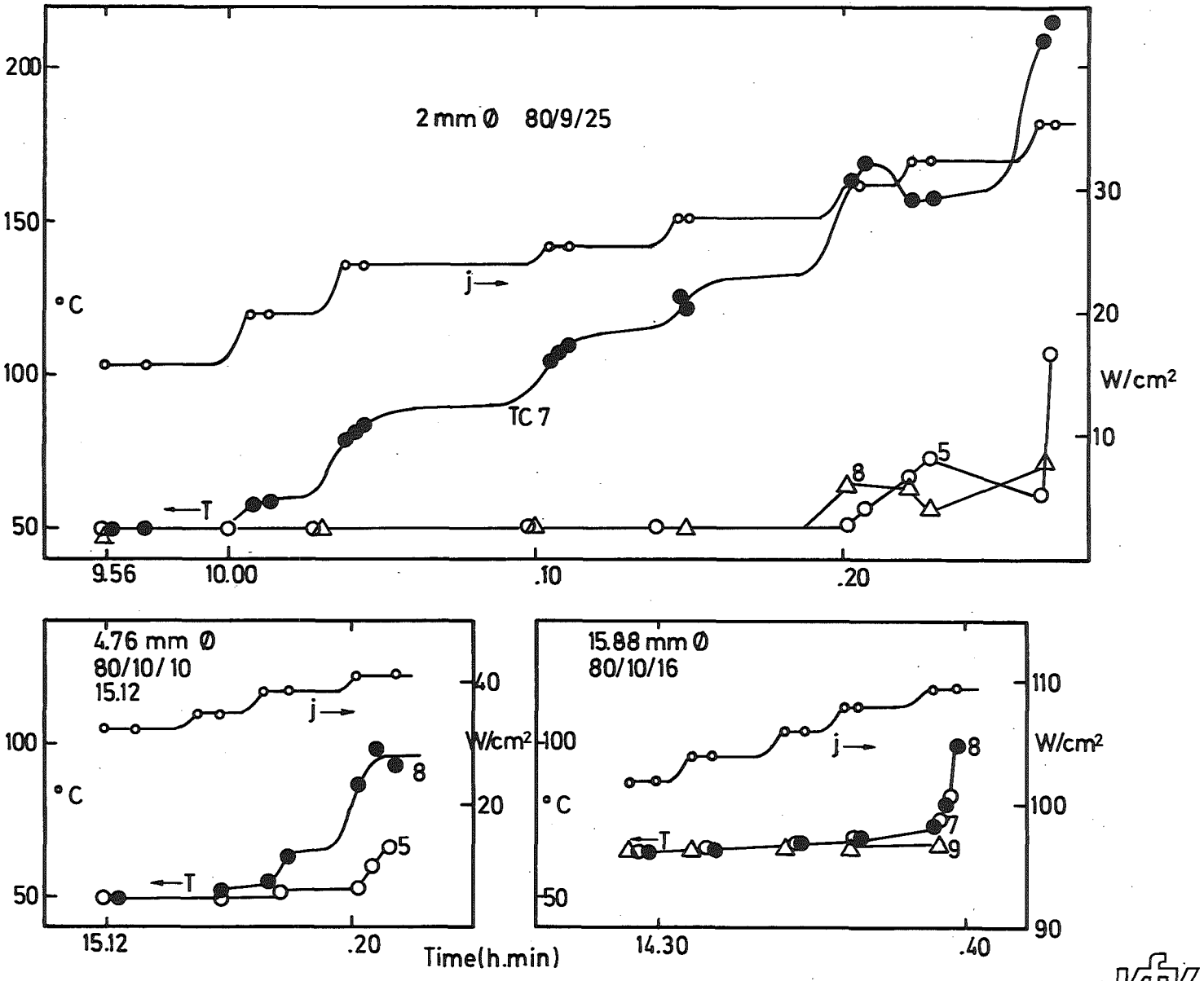

Fig. 6 Variation of heat flux j and bed temperature T with time for volume-heated stainless steel spheres in Freon-113

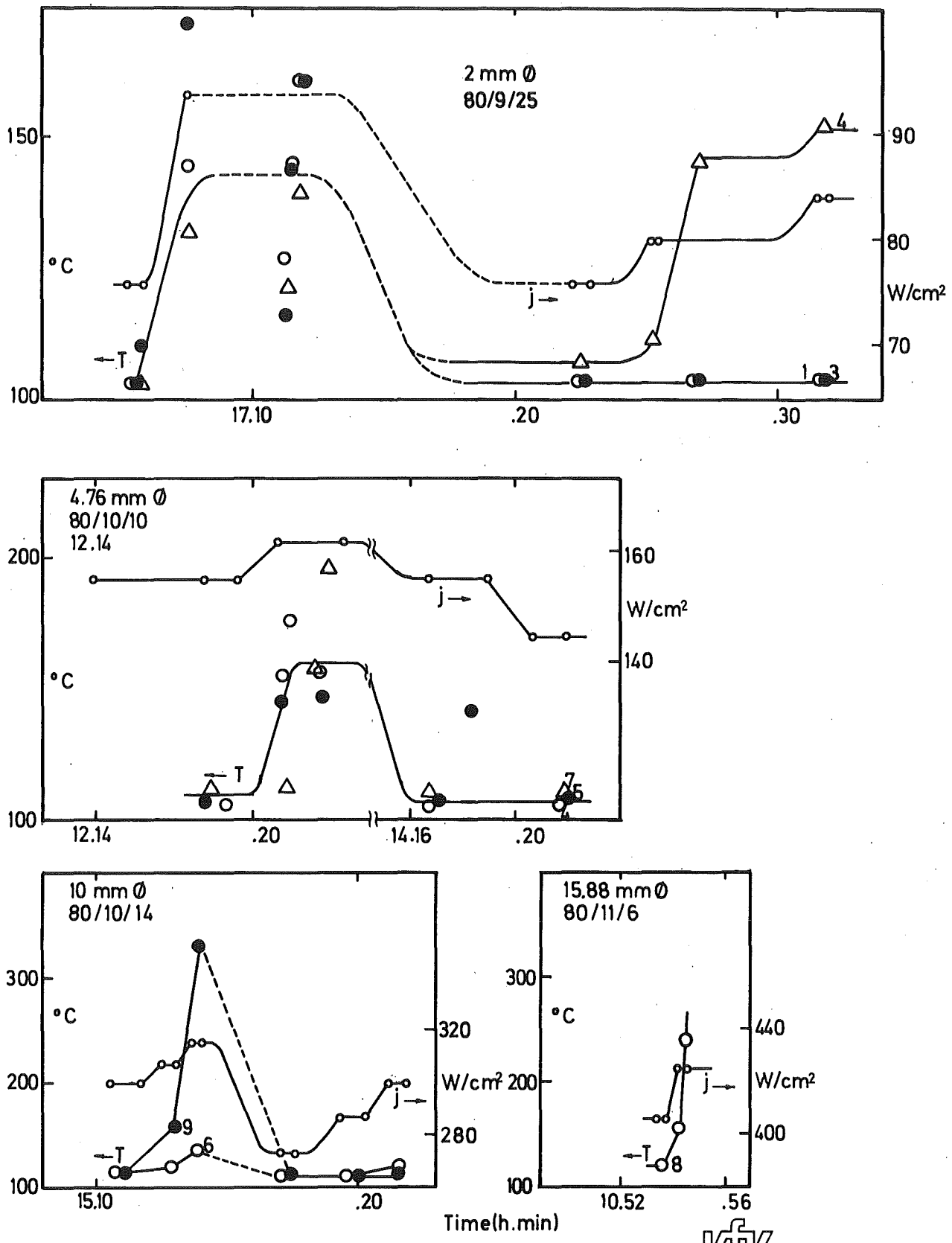

Fig. 7 Variation of heat flux j and bed temperature T with time for volume-heated stainless steel spheres in water

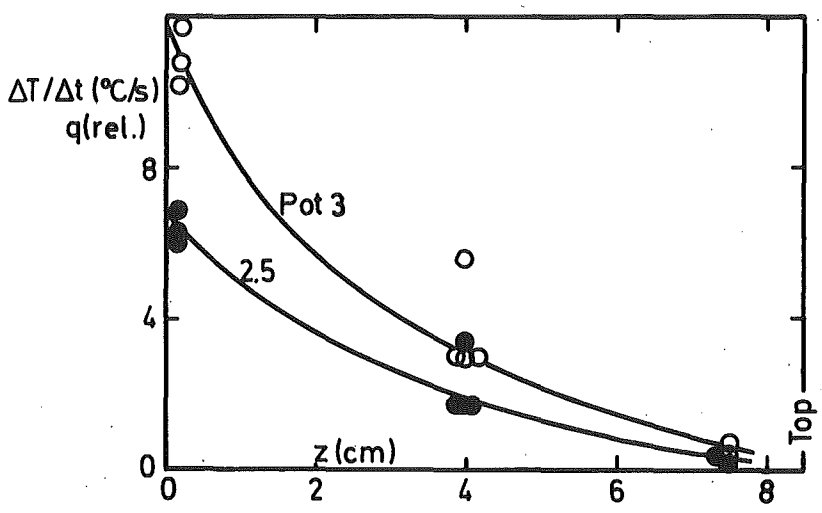

Fig. 8 Vertical power density distribution in "bottom heated" beds of 7.94 mm diameter stainless steel spheres (Run 80/10/13)

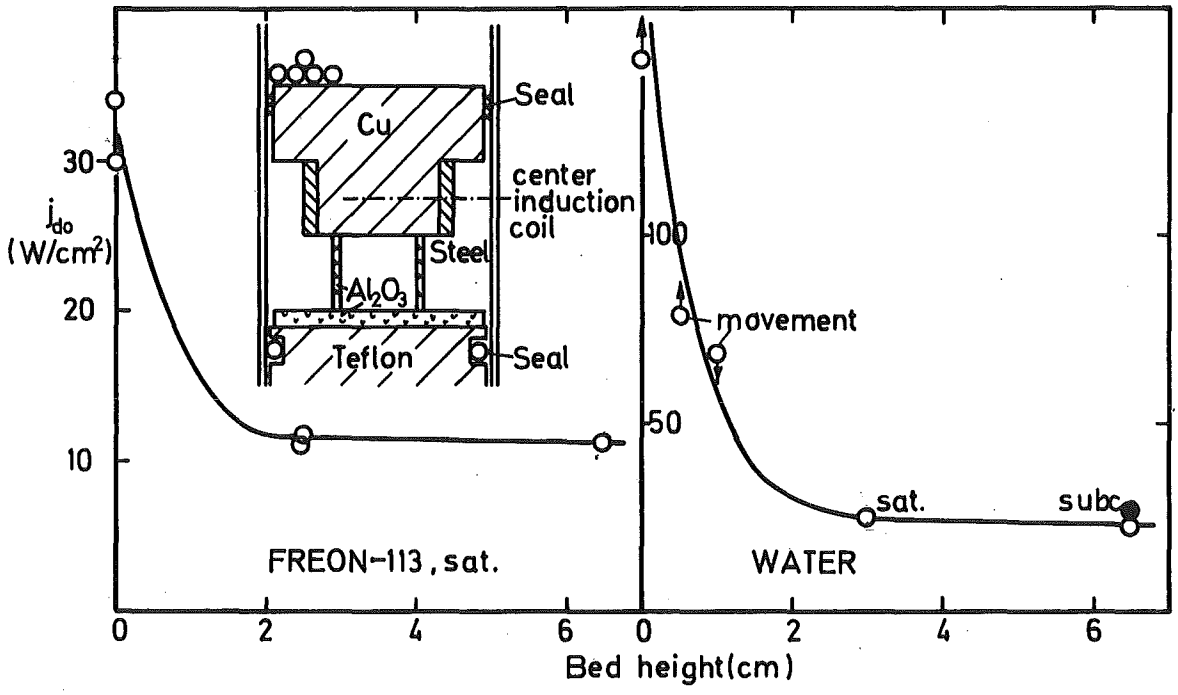

Fig. 9 Dryout heat fluxes for bottom-heated beds of 5.2 mm diameter glass spheres (for bed height ≥ 2.5 cm heat fluxes are normalized to $\varepsilon = 0.40$)

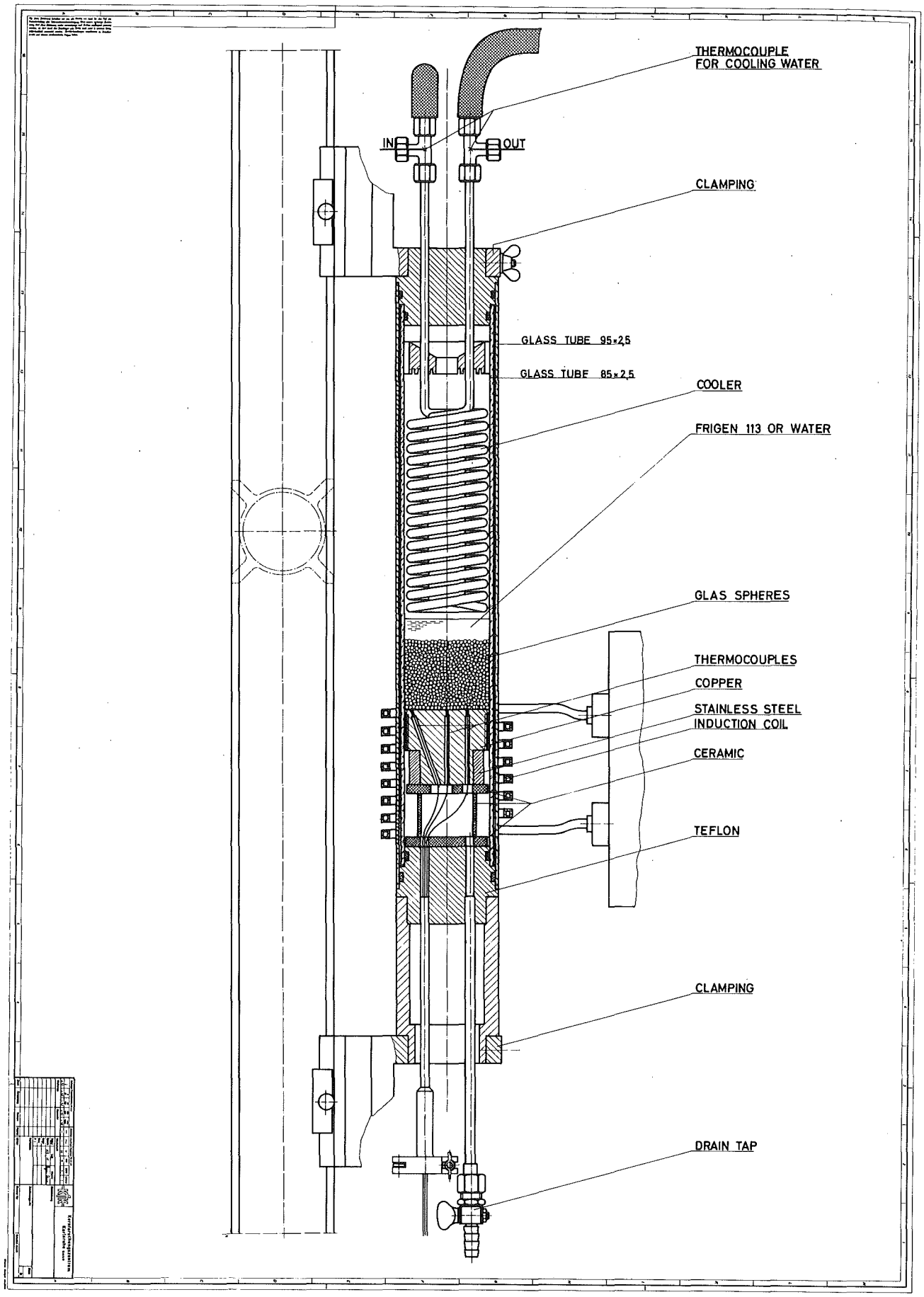

Fig. 10 Set-up for bottom-heating with copper plate

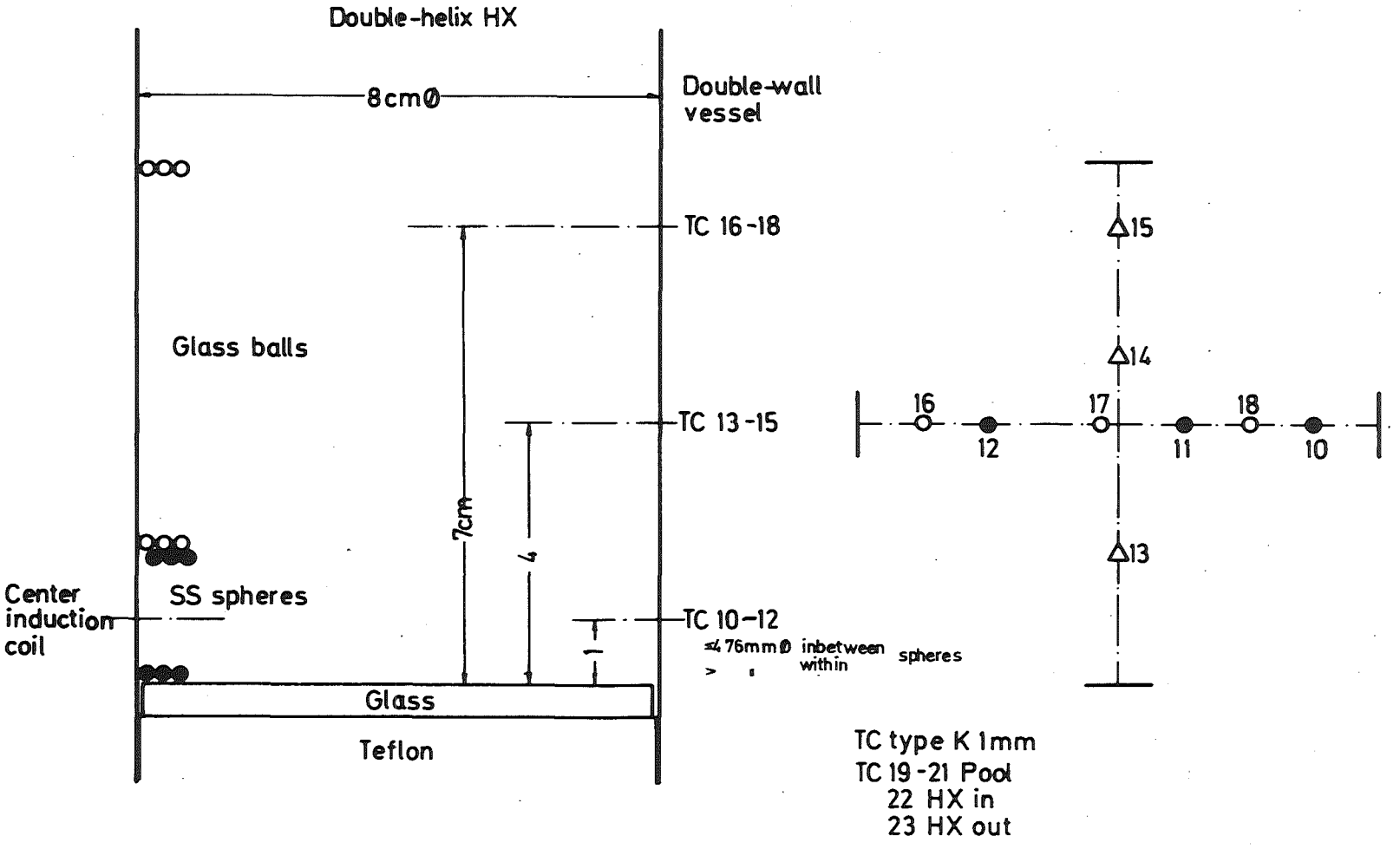

Fig. 11 Set-up for beds of glass balls heated by a shallow layer of stainless steel spheres

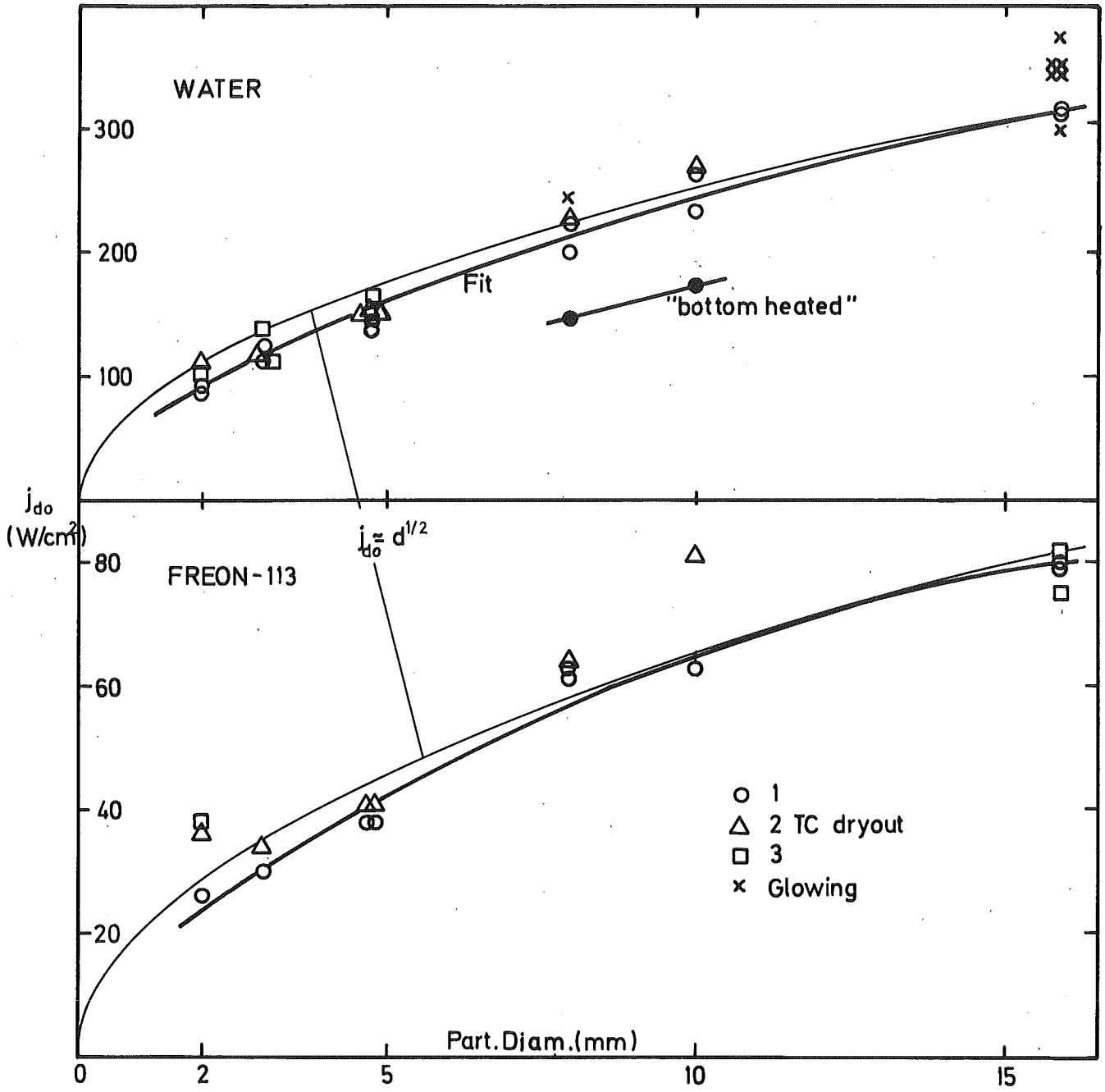

Fig. 12 Dryout heat fluxes for volume-heated beds of stainless steel spheres(adiabatic bottom, saturated conditions at atmospheric pressure, void fraction ε = 0.40, bed height 6-9 cm)

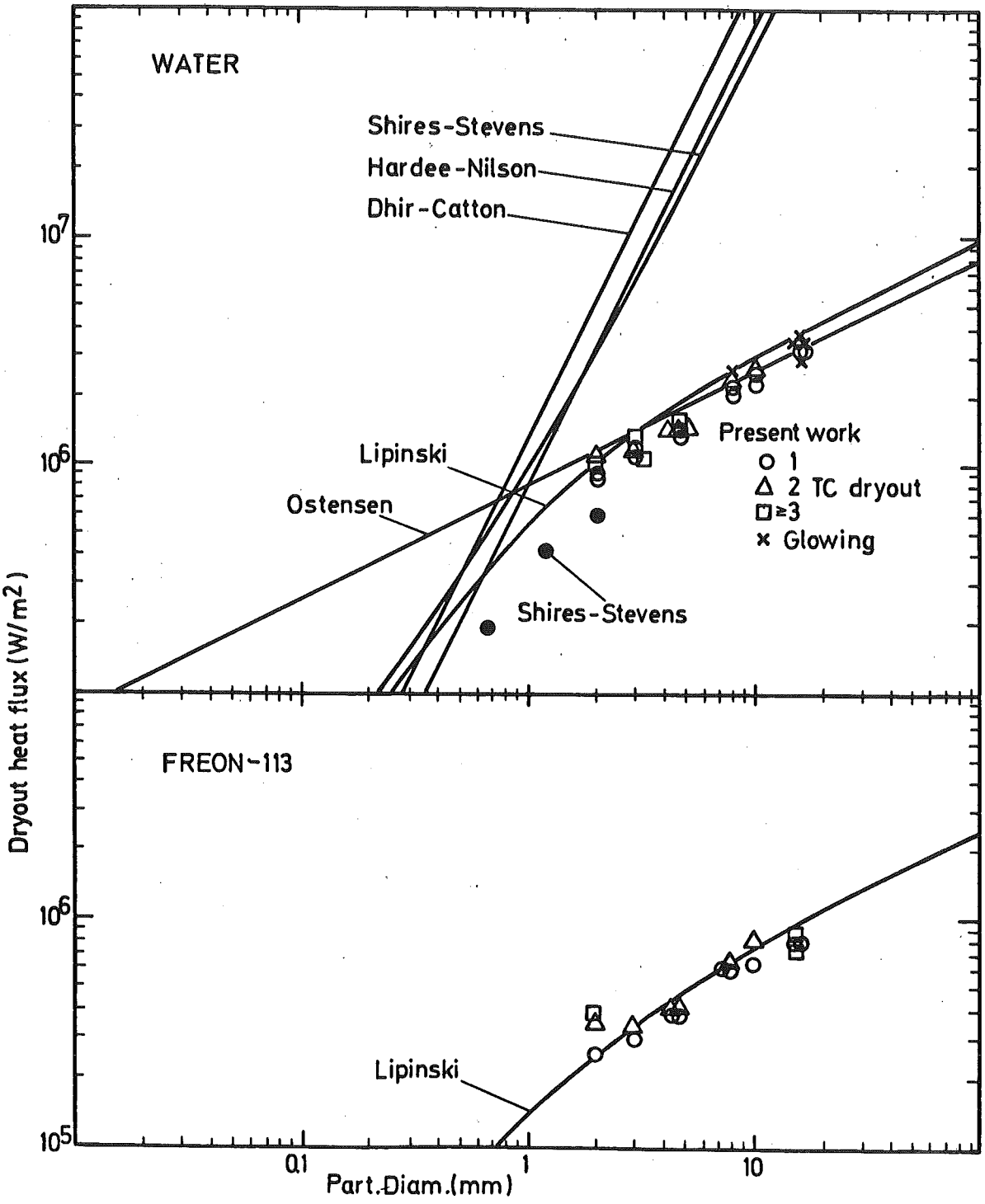

Fig. 13 Comparison of experimental (points, bed height 6-9 cm) and theoretical (curves, bed height 10 cm) volume-heated dryout heat fluxes (bottom adiabatic, saturated conditions at atmospheric pressure, void fr action $\varepsilon = 0.40$)

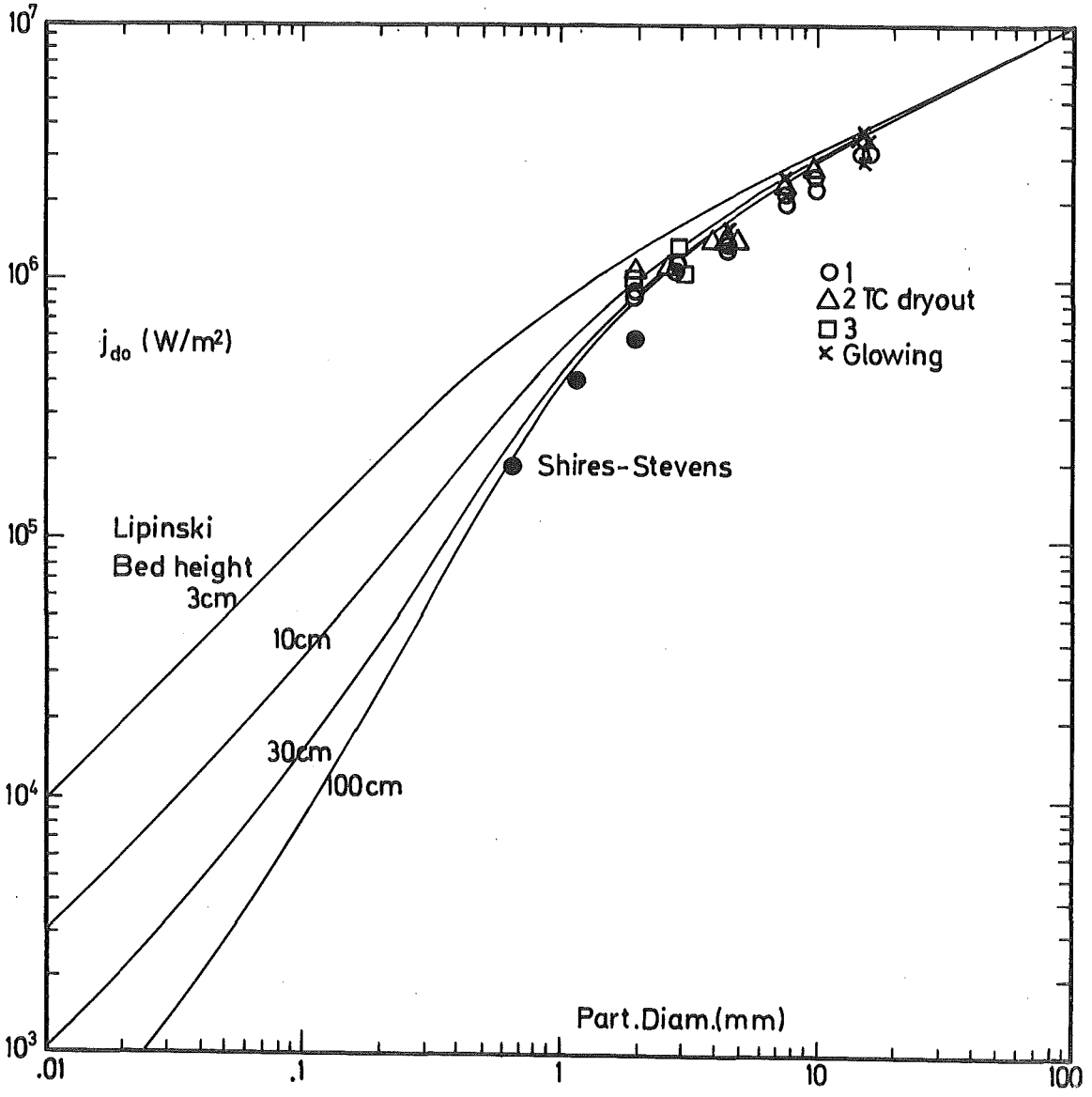

Fig. 14 Comparison of experimental (points, bed height 6-9 cm) volume-heated dryout heat fluxes with Lipinski's prediction (curves) /5/ for water (bottom adiabatic, saturated conditions at atmospheric pressure, void fraction $\varepsilon = 0.40$)

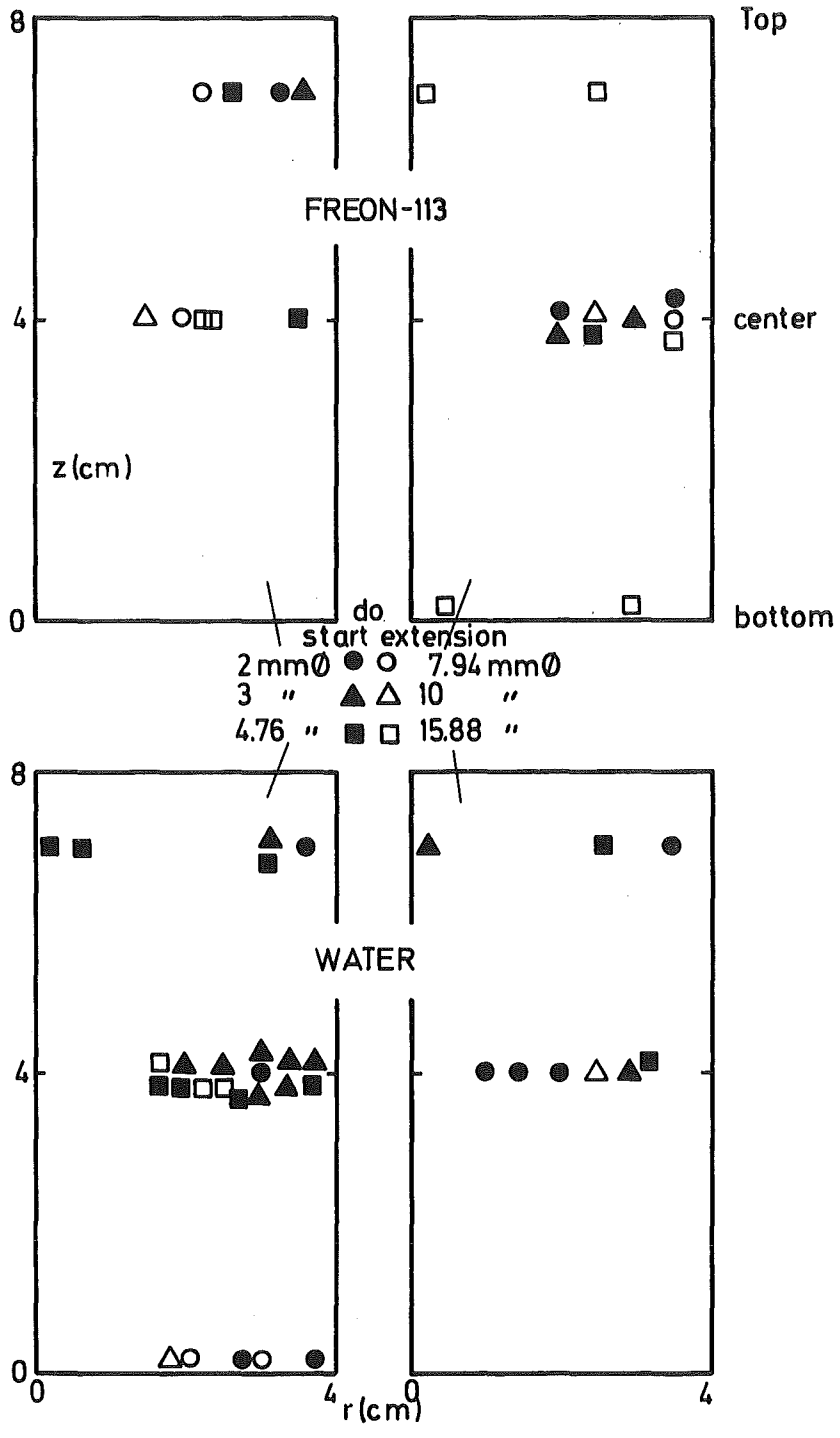

Fig. 15 Location of the dryout zone in volume-heated beds (bottom adiabatic) of stainless steel spheres (black symbols: first dryout, open symbols: extension of dryout)

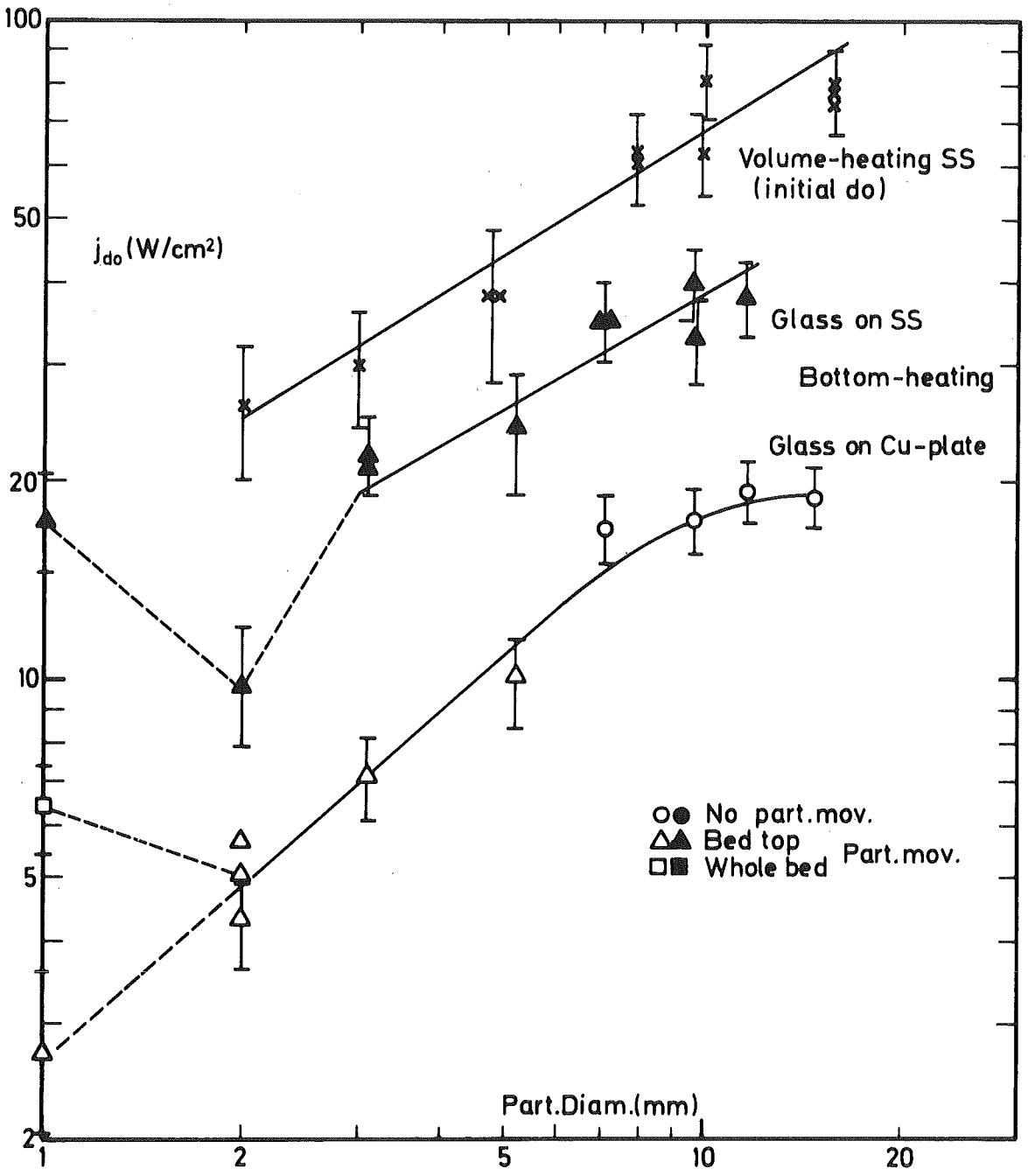

Fig. 16 Comparison of volume- and bottom-heated dryout heat fluxes for Freon-113 (saturated conditions at atmospheric pressure, void fraction ε = 0.40, bed height 6 - 9 cm)

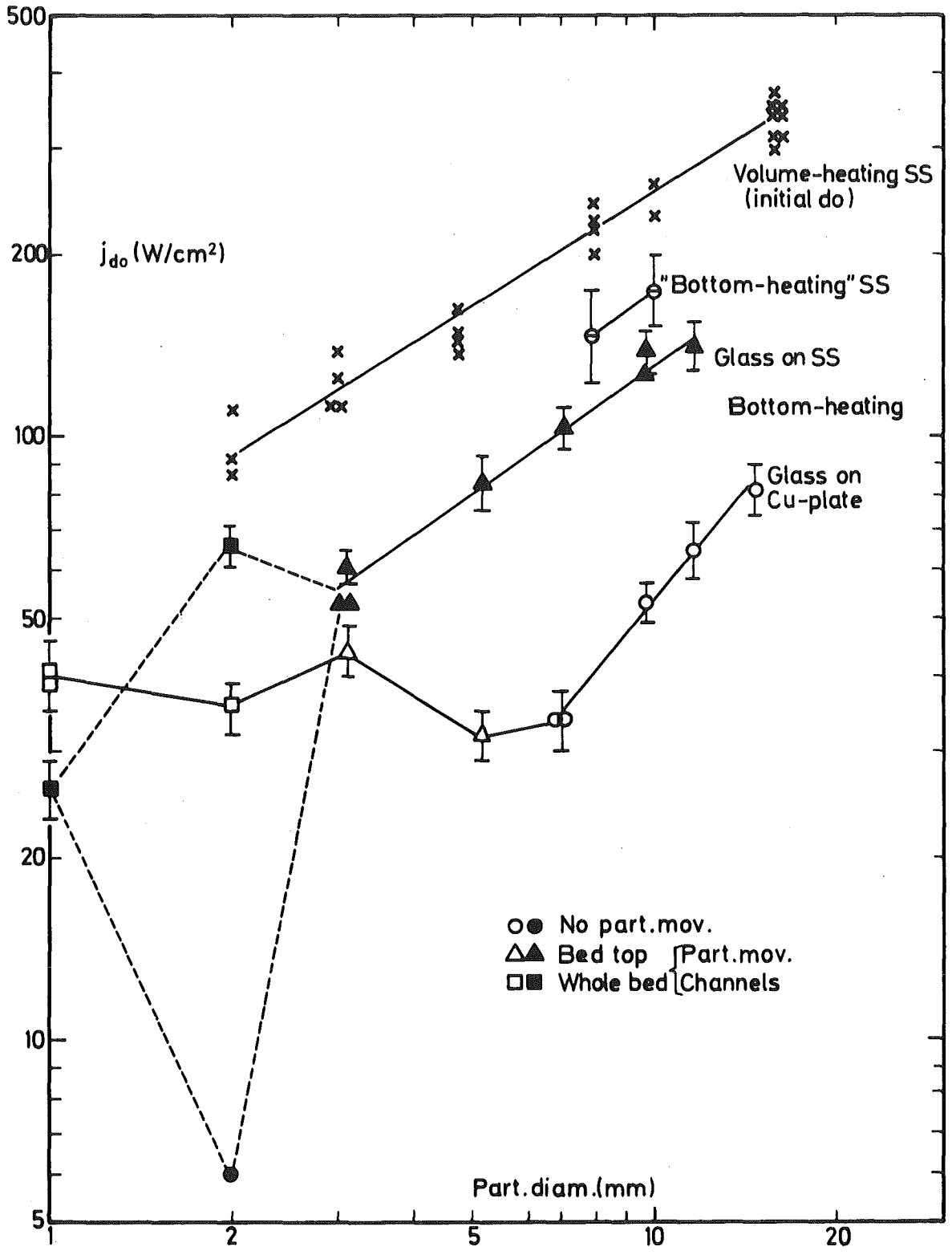

Fig. 17 Comparison of volume- and bottom-heated dryout heat fluxes for water (saturated conditions at atmospheric pressure, void fraction ε = 0.40, bed height 6 - 9 cm)